Journal of Thermal Analysis and Calorimetry, Vol. 79 (2005) 425–428

ACID PROPERTIES OF AlMCM-41 MOLECULAR SIEVES WITH DIFFERENT SILICA–ALUMINA RATIOS BY THERMOGRAVIMETRY

M. J. B. Souza[1], *A. O. S. Silva*[1], *V. J. Fernandes Jr.*[2] *and A. S. Araujo*[2*]

[1]Federal University of Rio Grande do Norte, Department of Chemical Engineering, 59078-970 Natal, RN, Brazil
[2]Federal University of Rio Grande do Norte, Department of Chemistry, CP 1662, 59078-970 Natal, RN, Brazil

A series of AlMCM-41 molecular sieves were synthesized starting from a hydrogel keeping the following molar composition: 1CTMABr:4.58SiO_2:(0.437+*X*)Na_2O:*X*Al_2O_3:200H_2O. Tetramethylammonium silicate (TMAS) was used as silicon source and cethyltrimethylammonium bromide (CTMABr) was used as structure template. The obtained materials were characterized by nitrogen adsorption, XRD and TG/DTG. Acid properties were determined by pyridine thermodesorption. Model-free and Flynn–Wall kinetic models were used in order to correlate the total acidity with the apparent activation energy of pyridine desorption.

Keywords: *acidity, AlMCM-41, pyridine, Si/Al ratio*

Introduction

The M41S materials are very important class of nanostructured materials due their potential applications in catalytic and adsorption processes. The MCM-41 silica which pore structure consists of hexagonally packed cylindrical particles is the main component of the M41S family [1, 2]. The hexagonal mesoporous systems with high surface area open possibilities to generate the surface acidity necessary to catalyze organic reactions in the petroleum industry. Studies involving the incorporation of aluminum in the structure of mesoporous materials can be visualized in [3, 4]. In this work a comparative study of the acidity properties of a series of AlMCM-41 materials with different silicon/aluminum ratios was performed. The results were correlated with model-free [5, 6] and Flynn–Wall [7] kinetic models in order to evaluate the influence of the silicon/aluminum ratio and total acidity through the apparent activation energy of pyridine desorption as function of the degree of desorption.

Experimental

The AlMCM-41 materials were synthesized starting from tetramethylammonium silicate (TMAS, Sigma-Aldrich) as silicon source, sodium hydroxide (VETEC) as sodium source, pseudobohemite (Vista) as aluminum source, cethyltrimethylammonium bromide (CTMABr, vetec) as template structure and distilled water as solvent. For the pH adjustment, 30% acetic acid in ethanol solution was used. The chemicals were mixed in order to obtain a gel with the following molar composition: 4.58SiO_2:(0.437+*X*)Na_2O:1CTMABr: *X*Al_2O_3:200H_2O. The value of *X* represents the molar coefficient to the aluminum source. The values of *X* were 0.114, 0.0570, 0.0380 and 0.0285 in order to obtain materials with 20, 40, 60 and 80 silicon/aluminum atomic ratios, respectively. The hydrogels were placed into 45 mL teflon-lined autoclaves and heated at 100°C for three days. Their pH was measured each day and was adjusted to 9–10. In the last day sodium acetate (Carlo Erba) was added to reach a 1:3 molar ratio between CH_3COONa/CTMABr in order to stabilize the silica [8]. The obtained materials were filtered, washed and dried at 100°C in an oven at 100°C for 2 h. The materials were calcinated at 450°C for one hour in nitrogen and for an additional hour in air at a heating rate of 5°C min^{-1} (both flow rates were 100 mL min^{-1} in agreement with [9, 10]). Acid form of AlMCM-41 materials was obtained by two successive reflux of ca. 0.5 g of each material with 0.6 M solution of NH_4Cl by 2 h at 60°C followed by calcination at 450°C in nitrogen atmosphere for 1 h. The pyridine adsorption experiments on the HAlMCM-41 samples were performed in a reactor containing ca. 0.1 g of catalyst, which was activated initially at 400°C, under nitrogen (flow rate: 100 mL min^{-1}) for 2 h. After this activation, the temperature was reduced to 95°C and the nitrogen flow was passed through in a bubbler flask containing liquid pyridine. The pyridine saturated nitrogen stream went through the reactor containing the samples, for 40 min. After then, pure nitrogen was passed through again over the samples for 40 min more in order to remove the physically adsorbed pyridine.

* Author for correspondence: asa-ufrn@usa.net

1388–6150/$20.00

Akadémiai Kiadó, Budapest, Hungary
Springer, Dordrecht, The Netherlands

XRD measurements were carried out in Shimadzu equipment using CuK_α radiation in 2θ degree of 1 to 10° with a step of 0.01°. Surface area, pore volume and pore distribution were obtained by BET [11] and BJH [12] methods stating of nitrogen adsorption isotherms at 77 K (ANOVA 2000). TG analysis was carried out using a Mettler TGA/SDTA851 equipment and nitrogen purging with a flow rate of 25 mL min^{-1}. The samples as synthesized were heated from room temperature up to 900°C, at a heating rate of 5, 10 and 20°C min^{-1}. The Vyazovkin [5, 6] and Flynn–Wall [7] kinetic models were used to determine the apparent activation energy as a function of the pyridine degree desorption.

Results and discussion

Figure 1 shows the XRD powder patterns of the calcined AlMCM-41 samples obtained with different silicon/aluminum ratios after calcination of the as-synthesized samples.

From the XRD measurements it can be observed that the intensity of the diffraction patterns significantly decreased with the increasing of the silicon/aluminum ratios with exception of the sample obtained with Si/Al ratio of 40. The variation in the XRD intensities is attributed to obtaining of samples with different crystallinity degrees, which is a known behavior related to the increase of contrast between the silica–aluminum wall and the pore diameter after the removal of the surfactant [13]. Papers report that the incorporation of aluminum in the MCM-41 materials provokes higher degrees of crystallinity than pure siliceous MCM-41 due to the larger structure stability of the obtained materials [14, 15]. All the samples showed characteristic peaks in the 2θ ranges of 1 to 10°, related to (100), (110), (210) Miller indices, characteristics of AlMCM-41 materials [1, 2]. The specific surface area was determined according to the standard Brunauer–Emmett–Teller (BET) method [11] and pore size distributions by Barrett–Joyner–Halenda (BJH) algorithm [12]. The adsorption parameters are collected in Table 1. Surveying the data of Table 1 one can notice that there are samples with remarkable specific surface area, pore volume and silica–alumina wall thickness. These properties are depending on the degree of crystallinity as it is shown in Fig. 1. Samples with high degree of crystallinity present the highest degree of hexagonal ordination and consequently high values of specific surface area, pore diameters and pore volumes.

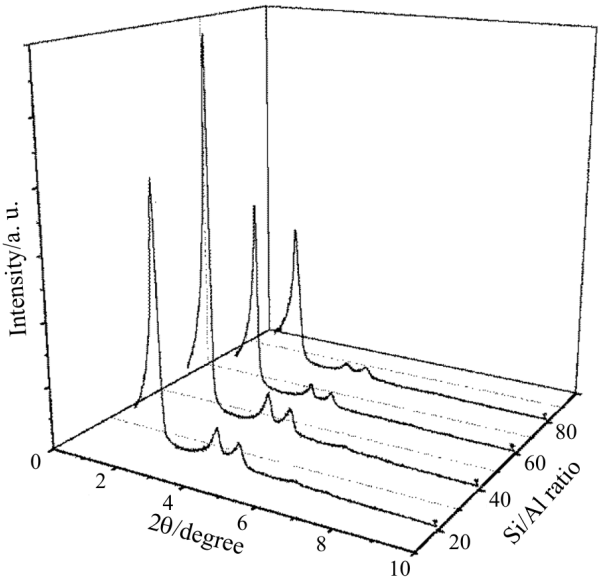

Fig. 1 XRD powder patterns of AlMCM-41 with different silicon/aluminum ratios

TG analysis of pyridine adsorbed on HAlMCM-41 materials showed typically 2 mass losses. The first one is between 30–100°C and was attributed to the evaporation of water and physisorbed pyridine. The second one appeared between 100–260°C representing the release of chemisorbed pyridine in the HAlMCM-41 acid centers. The relative temperature range of pyridine desorption in comparison with experiments performed on zeolites using similar bases [16–18] suggests that the acid centers possess weak-medium strength. The total acidity was measured starting from the mass losses of chemisorbed pyridine (X_{pir}) from the materials in the temperature range of 100–260°C keeping in one's mind that each pyridine molecule adsorbs only in one acid center. Table 2 contains the mass losses taken from the TG curves of the HAlMCM-41 samples with different Si/Al ratios.

Table 1 Adsorption parameters for the AlMCM-41 samples

Sample	S_{BET}/m^2 g^{-1}	V_t/cm^3 g^{-1}	a_0/nm*	*Dp*/nm	*Wt*/nm**
AlMCM-41 (20)	803	0.47	4.18	2.32	1.86
AlMCM-41 (40)	894	0.58	4.16	2.59	1.57
AlMCM-41 (60)	658	0.38	4.23	2.12	2.11
AlMCM-41 (80)	525	0.35	4.39	2.72	1.67

*$a_0=2d_{(100)}/\sqrt{3}$ and **$Wt=a_0-Dp$

In order to evaluate the activation energy of pyridine desorption of HAlMCM-41 materials, other TG experiments were performed at 5 and 20°C min^{-1} heating rates. Taking in consideration that the pyridine desorption plots of logβ *vs*. $1000/T_\alpha$ (Fig. 2) and $\ln(\beta / T_\alpha^2)$ *vs*. $1000/T_\alpha$ (Fig. 3) were performed obtaining the apparent activation energy by Flynn–Wall (Eq. (1)) and model-free (Eq. (2)) kinetic models, respectively. As it can be observed in Table 2, with an increase in the Si/Al ratio occurred together with a decrease in the total acidity obtaining values of 1.2, 0.93, 0.82 and 0.43 mmol g^{-1} for Si/Al ratios of 20, 40, 60 and 80, respectively. The SiMCM-41 presents too a small superficial acidity (ca. 0.11 mmol g^{-1}) which is probably due to structural defects and non-condensed superficial silanol groups. The kinetic analysis by Flynn–Wall and model-free methods showed almost identical results and in all cases was observed that with the increase of Si/Al ratio an increase in the apparent activation energy occurred (Fig. 4), which is necessary to desorb the pyridine from the acidic sites. These results suggest that the high aluminum concentrations increase the total acidity but the relative force of those acid sites is committed and it tends to decrease.

$$E_a \cong -18.2 \frac{\partial(\log \beta)}{\partial(1/T)} \quad (1)$$

$$\ln \frac{\beta}{T_\alpha^2} = \ln\left[\frac{Rk_0}{E_\alpha g(\alpha)}\right] - \frac{E_\alpha}{R}\frac{1}{T_\alpha} \quad (2)$$

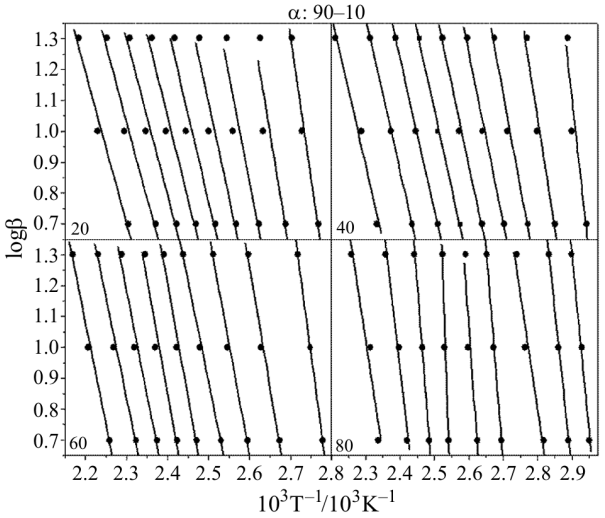

Fig. 2 Kinetic curves of pyridine desorption from AlMCM-41 with 20, 40, 60 and 80 Si/Al ratios obtained by Flynn–Wall kinetic model

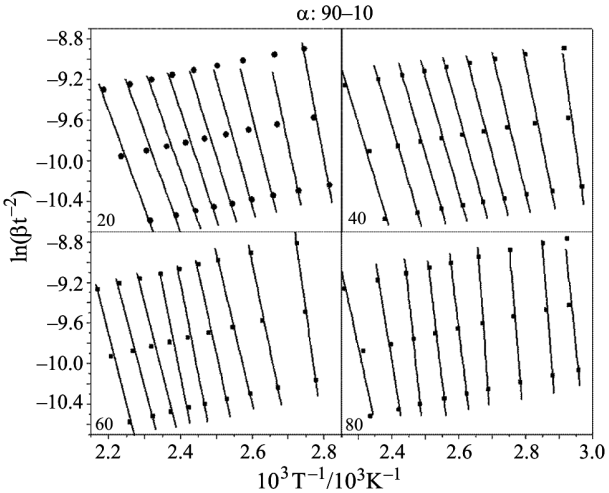

Fig. 3 Kinetic curves of pyridine desorption from AlMCM-41 with 20, 40, 60 and 80 Si/Al ratios obtained by model-free kinetic model

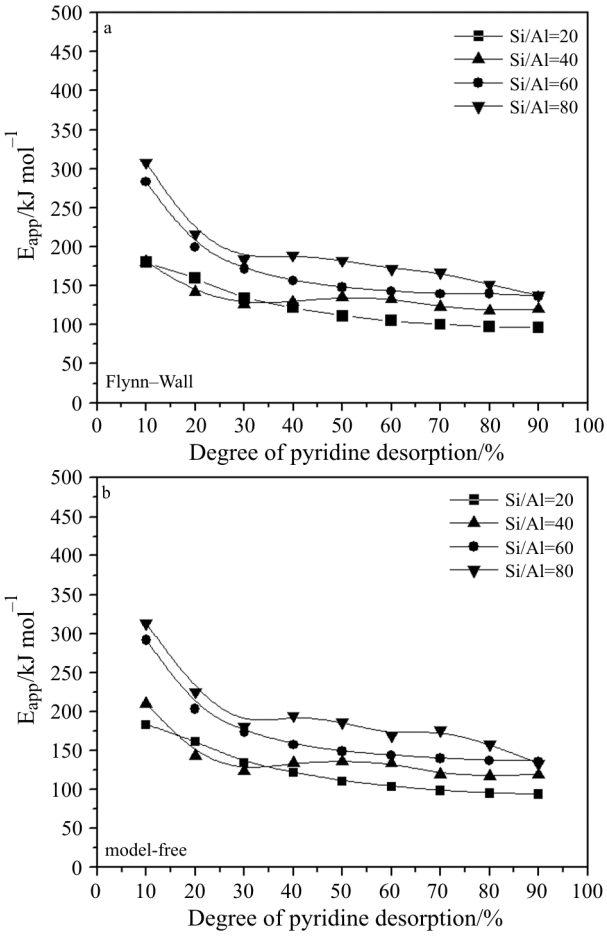

Fig. 4 Apparent activation energy curves *vs*. the degree of desorption of pyridine obtained by a – Flynn–Wall and b – model-free kinetic models

Table 2 Total acidity, mass losses (%) and respective temperatures ranges of pyridine desorption of HAlMCM-41 samples with different Si/Al ratios

Sample	Temperature range/°C			Total acidity/mmol g^{-1}*
	30–100	100–260	30–260	
HAlMCM-41 (20)	3.63	1.20	4.83	1.20
HAlMCM-41 (40)	3.48	0.93	4.41	0.93
HAlMCM-41 (60)	3.43	0.82	4.25	0.82
HAlMCM-41 (80)	5.09	0.43	5.52	0.43
**SiMCM-41	2.12	0.11	2.23	0.11

*data taken from [17]
**synthesized and characterized in [9]

Conclusions

In this work one can observe that the synthesis of MCM-41 with aluminum generates the AlMCM-41 aluminosilicate. Using pyridine as test molecule was satisfactory to evaluate the total acidity. For 20, 40, 60 and 80 Si/Al atomic ratios 1.2, 0.93, 0.82 and 0.43 mmol g^{-1} of total acidity values were obtained, respectively. Model-free and Flynn–Wall kinetic models were applied to determine the apparent activation energy of pyridine desorption. In all cases it was observed that with the increase of Si/Al ratio the apparent activation energy increased. These results suggest that the high aluminum concentrations increase the total acidity but decrease the relative acidity force of those acid sites.

Acknowledgements

The authors acknowledge the support from the Agência Nacional do Petróleo (MCT/PRH/ANP-14), FINEP/CTPetro and Conselho Nacional de Desenvolvimento Científico e Tecnológico (CNPq, Proc. 300.291/93).

References

1 X. S. Zhao, G. Q. Lu and G. J. Millar, Ind. Chem. Res., 35 (1996) 2075.
2 J. S. Beck, J. C. Vartuli, W. J. Roth, M. E. Leonowicz, C. T. Kresge, K. D. Schmitt, C. T. W. Chu, D. H. Olson, E. W. Sheppard, S. B. McCullen, Y. B. Higgins and I. L. Schelenker, J. Am. Chem. Soc., 114 (1992) 10834.
3 M. Busio, J. Janchen and J. H. C. Van Hoff, Microporous Mesoporous Mater., 5 (1995) 211.
4 Y. Cesteros and G. L. Haller, Microporous Mesoporous Mater., 43 (2001) 171.
5 S. Vyazovkin and A. I. Lesnikovich, Russ. J. Phys. Chem., 62 (1988) 2949.
6 S. Vyazovkin and V. Goryachko, Thermochim. Acta, 194 (1992) 221.
7 J. H. Flynn and L. S. Wall, Polym. Lett., 4 (1966) 323.
8 A. S. Araujo and M. Jaroniec, Thermochim. Acta, 363 (2000) 175.
9 M. J. B. Souza, A. O. S. Silva, J. M. F. B. Aquino, V. J. Fernandes Jr. and A. S. Araujo, J. Therm. Anal. Cal., 75 (2004) 693.
10 A. S. Araujo, V. J. Fernandes Jr., M. J. B. Souza, A. O. S. Silva and J. M. F. B. Aquino, Thermochim. Acta, 413 (2004) 235.
11 S. Brunauer, P. H. Emmett and J. Teller, J. Am. Chem. Soc., 60 (1938) 309.
12 E. P. Barret, L. J. Joyner and P. Halenda, J. Am. Chem. Soc., 73 (1951) 373.
13 B. Marler, U. Oberhagemann, S. Vortmann and H. Gies, Microporous Mesoporous Mater., 6 (1996) 375.
14 S. C. Shen and S. Kavi, J. Phys. Chem. B., 103 (1999) 8870.
15 A. S. Araujo, C. D. R. Souza, M. J. B. Souza, V. J. Fernandes Jr. and L. A. M. Pontes, Stud. Surf. Sci. Catal., 141 (2002) 467.
16 T. J. G. Kofke, R. J. Gorte, G. T. Kokotailo and W. E. Farneth, J. Catal., 115 (1989) 265.
17 A. S. Araujo, V. J. Fernandes and S. A. Veríssimo, J. Therm. Anal. Cal., 59 (2000) 649.
18 A. O. S. Silva, M. J. B. Souza, J. M. F. B. Aquino, V. J. Fernandes Jr. and A. S. Araujo, J. Therm. Anal. Cal., 75 (2004) 699.